

# Current Biology

## Auditory Sensitivity and Decision Criteria Oscillate at Different Frequencies Separately for the Two Ears

### Highlights

- We report for the first time oscillations in auditory perception
- Oscillations occurred in both sensitivity (~6 Hz) and decision criterion (~8 Hz)
- Sensitivity oscillated between the two ears in antiphase
- Rhythmic oscillations are a general phenomenon of many aspects of perception

### Authors

Hao Tam Ho, Johahn Leung,  
David C. Burr, David Alais,  
Maria Concetta Morrone

### Correspondence

tam.ho@sydney.edu.au (H.T.H.),  
dave@in.cnr.it (D.C.B.)

### In Brief

Using signal detection theory, Ho et al. report that both perceptual sensitivity and decision criterion oscillate in audition (at 6 Hz and 8 Hz, respectively). The oscillations in sensitivity suggest alternate sampling of the two ears by attention-like mechanisms. Rhythmic oscillations seem to be a general phenomenon of many aspects of perception.

# Auditory Sensitivity and Decision Criteria Oscillate at Different Frequencies Separately for the Two Ears

Hao Tam Ho,<sup>1,3,\*</sup> Johahn Leung,<sup>1,2</sup> David C. Burr,<sup>1,5,6,\*</sup> David Alais,<sup>1</sup> and Maria Concetta Morrone<sup>3,4</sup>

<sup>1</sup>School of Psychology, University of Sydney, Brennan MacCallum Building A18, Manning Road, Camperdown, NSW 2006, Australia

<sup>2</sup>School of Medical Sciences, University of Sydney, Anderson Stuart Building, F13 Eastern Avenue, NSW 2006, Australia

<sup>3</sup>Department of Translational Research on New Technologies in Medicine and Surgery, University of Pisa, Via San Zeno 31, 56123 Pisa, Italy

<sup>4</sup>Scientific Institute Stella Maris, Viale del Tirreno, 331, 56018 Calambrone, Pisa, Italy

<sup>5</sup>Department of Neuroscience, Psychology, Pharmacology, and Child Health, University of Florence, Via di San Salvi 12, 50139 Florence, Italy

<sup>6</sup>Lead Contact

\*Correspondence: [tam.ho@sydney.edu.au](mailto:tam.ho@sydney.edu.au) (H.T.H.), [dave@in.cnr.it](mailto:dave@in.cnr.it) (D.C.B.)

<https://doi.org/10.1016/j.cub.2017.10.017>

## SUMMARY

Many behavioral measures of visual perception fluctuate continually in a rhythmic manner, reflecting the influence of endogenous brain oscillations, particularly theta (~4–7 Hz) and alpha (~8–12 Hz) rhythms [1–3]. However, it is unclear whether these oscillations are unique to vision or whether auditory performance also oscillates [4, 5]. Several studies report no oscillatory modulation in audition [6, 7], while those with positive findings suffer from confounds relating to neural entrainment [8–10]. Here, we used a bilateral pitch-identification task to investigate rhythmic fluctuations in auditory performance separately for the two ears and applied signal detection theory (SDT) to test for oscillations of both sensitivity and criterion (changes in decision boundary) [11, 12]. Using uncorrelated dichotic white noise to induce a phase reset of oscillations, we demonstrate that, as with vision, both auditory sensitivity and criterion showed strong oscillations over time, at different frequencies: ~6 Hz (theta range) for sensitivity and ~8 Hz (low alpha range) for criterion, implying distinct underlying sampling mechanisms [13]. The modulation in sensitivity in left and right ears was in anti-phase, suggestive of attention-like mechanisms sampling alternatively from the two ears.

## RESULTS

The phase of ongoing neural oscillations can be reset using salient visual cues [2, 3, 14, 15] or eye or arm movements [1, 16, 17], causing visual performance (both accuracy and reaction times) to oscillate within the lower alpha and upper theta bands (4–8 Hz). We hypothesized that oscillations in the auditory system could be also reset by the onset of an auditory burst. We presented participants with a stream of dichotic uncorrelated white noise and asked them to identify the pitch of a brief

monaural target tone presented with equal probability to the left or right ear at random intervals from 0.2 to 1.01 s after the noise onset (Figure 1). For the aggregate subject data analysis, we pooled across all participants' responses (separate for left ear and right ear) and binned the data with rectangular, non-overlapping windows of 19.5 ms. For each bin, we computed sensitivity,  $d'$ , and criterion,  $c$ , using Equations 1 and 2 (see Quantification and Statistical Analysis in STAR Methods). The group means for  $d'$  across all bins are 1.06 ( $\pm 0.08$  SD) and 1.05 ( $\pm 0.06$ ) for the left ear and right ear, respectively, and the group means for  $c$  are  $-0.14$  ( $\pm 0.23$ ) and  $-0.08$  ( $\pm 0.20$ ). The results of the individual subject analysis are shown in Figures S1–S4 (see Supplemental Information).

Figures 2A and 2C show the detrended sequences of the left- and right-ear sensitivities (blue lines) as a function of target stimulus-onset asynchrony (SOA) from noise onset. The black curves represent the best sinusoidal fits to the data (Equation 3; see Quantification and Statistical Analysis in STAR Methods). For the left ear, this is 6.2 ( $\pm 0.4$ ) Hz, and for the right ear, it is 5.7 ( $\pm 0.3$ ) Hz. Figure 2E shows the goodness of fit ( $R^2$ ) of the sensitivity data of the two ears for all frequencies within the sampled range (4–10 Hz, in steps of 0.1 Hz). The  $R^2$ s at the peak frequencies—6.2 for the left ear and 5.7 Hz for the right ear—are 0.3 ( $\pm 0.03$ , calculated by jack-knife) and 0.2 ( $\pm 0.03$ ), respectively, which are clearly higher than the 95<sup>th</sup> percentile of the  $R^2$  distribution obtained by permutation ( $n = 2,000$ ). The 95<sup>th</sup> percentile was essentially constant near  $R^2 = 0.15$  at all frequencies. For both ears, the goodness of fit of the binned data exceeded the 95% permutation threshold over a specific range of frequencies, 5.7–6.6 Hz for the left ear and 5.3–5.9 Hz for the right (Figure 2E, shaded rectangles). The two intervals clearly overlapped over the range of 5.7–5.9 Hz, suggesting a common generator of oscillations for sensitivity of the two ears.

Figures 2B and 2D show the criterion estimates for the aggregate subject data for the two ears (pink lines) as a function of SOA, with the best sinusoidal fits shown in black. The best fits for criteria were at higher frequencies than for sensitivity: 8.7 ( $\pm 0.7$ ) Hz for the left ear ( $R^2 = 0.2 \pm 0.02$ ) and 7.5 ( $\pm 0.5$ ) Hz for the right ( $R^2 = 0.3 \pm 0.04$ ). Figure 2F shows the range of frequencies where the modulation was greater than the

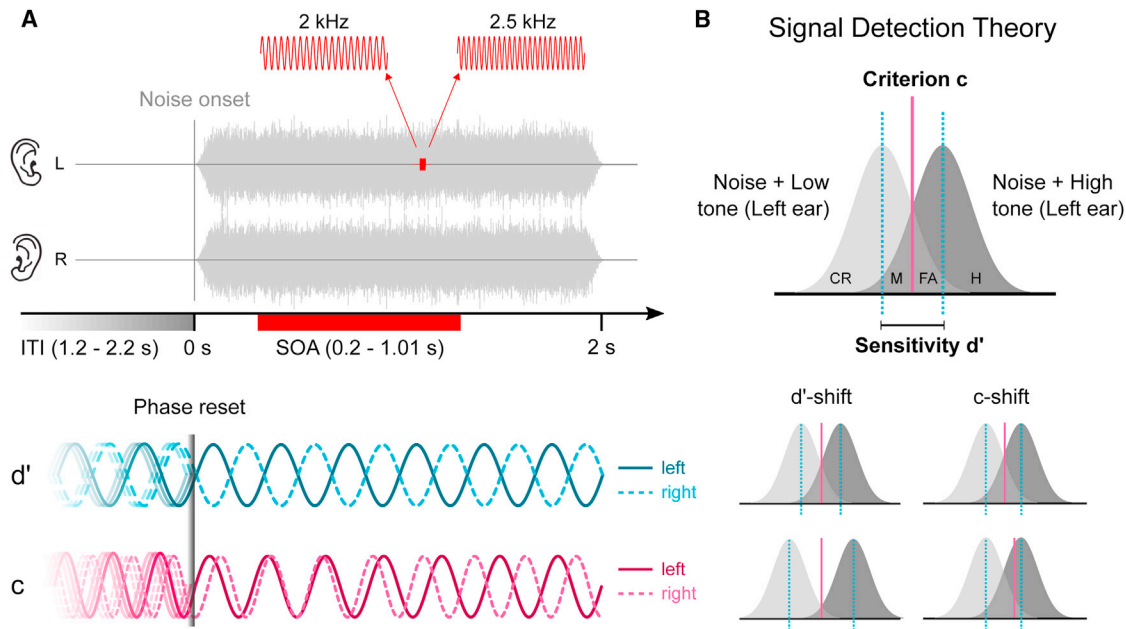


**Figure 1. Experimental Design and Application of Signal Detection Theory**

(A) Top: schematic of a trial. Each trial started with white noise presented for 2 s to both ears. A pure tone of either 2 kHz (low) or 2.5 kHz (high) and 10-ms duration was delivered with equiprobability to the left or right ear. The SOA was randomly selected from an interval of 0.2–1.01 s post-noise onset. The inter-trial interval (ITI) jittered randomly between 1.2 and 2.2 s. Bottom: phase reset by noise onset. We hypothesized that the noise onset resets the phase of ongoing oscillations. The light and dark blue sinusoids represent schematically the results for the sensitivity oscillations in the left and right ear, which fluctuate at a similar frequency but in antiphase (180°). The light and dark pink sinusoids represent schematically the criterion oscillations in the left and right ear, which fluctuate at different frequencies.

(B) Top: SDT application. We computed sensitivity ( $d'$ ) and criterion ( $c$ ) based on the hit rate (H) from the high-pitch tone condition and the false-alarm rate (FA) from the low-pitch tone condition for each ear (CR, correct rejection; M, miss). Bottom: illustrations of shifts in  $d'$  and  $c$ . The overlap between the two probability distributions determines the  $d'$  shift; the shift in decision boundary (pink line) to the left or the right determines the  $c$  shift.

95% permutation threshold. Unlike for sensitivity, the frequency ranges were non-overlapping for the criterion, with 8.4–8.9 Hz for the left ear and 7.1–7.9 Hz for the right.

The goodness of fit does not specify the strength of the observed oscillations, which can be evaluated by the amplitude and phase coherence of the sinusoidal fits. Figures 3A and 3E show the amplitude spectra of the sensitivity oscillations in the left and right ears over the same range of sampled frequencies (4–10 Hz). The amplitude spectra of the left- and right-ear criteria are shown in Figures 3C and 3G. The shading surrounding the blue (sensitivity) and pink (criterion) lines corresponds to  $\pm 1$  SEM, calculated by bootstrapping the original data. Supporting the goodness of fit of the criterion data in Figure 2F, the amplitude spectra suggest that the strongest oscillations of criterion were different between the two ears, with  $A = 0.04$  at 8.7 Hz for the left ear and  $A = 0.04$  at 7.5 Hz for the right. To evaluate the significance of both the phase and amplitude at these frequencies, we performed a two-dimensional (2D) analysis on the sine and cosine coefficients of the sinusoidal fit [1, 16]. In Figures 3D and 3H, the black dots indicate the response vectors (reflecting the amplitude and phase) of the aggregate subject at the peak frequencies, while the surrounding clouds of pink dots indicate the vectors for each bootstrap at that frequency. The amplitude is given by the distance from the origin, and phase is given by the angle of the vector. The gray shaded area encircling 95% of the colored points does not extend past

the origin in either case, indicating that the vector is significantly different from zero [1, 16]. We calculated the proportion of points that fall beyond the pink dashed lines passing through the origin and that are orthogonal to the original phase (dotted black lines) [18]. The resulting  $p$  values were corrected for multiple comparisons across all 61 frequencies of Figure 2F, using false discovery rate (FDR) [19]. Allowing for an FDR of 10% [20], the left-ear criterion was significant at 8.7 Hz,  $p = 0.003$ ; and the right-ear criterion was significant at 7.5 Hz,  $p = 0.002$ . All frequencies in the shaded gray area in Figures 3C–3G were significant after FDR correction. Our analysis of individual responses corroborated the phase coherence observed in the aggregate data, even though subjects' maximal frequency and amplitude varied (Figures S2 and S3). From a vector analysis of the group mean amplitudes and intersubject phase coherence, statistical significance can only be met when both are greater than the permuted data. For the left ear, this is true for participants' phases around 8.7 Hz ( $p = 0.05$ ), with a mean phase,  $\theta$ , of  $241^\circ$  ( $\pm 43^\circ$ ) and a mean vector length,  $|\nu|$ , of 0.03. For the right ear, participants' phases were most consistent around 7.5 Hz ( $p = 0.01$ ) with  $\theta = 146^\circ$  ( $\pm 36^\circ$ ) and  $|\nu| = 0.05$ .

Next, we examined the amplitude spectra of the oscillations in sensitivity (Figures 3A and 3E). In agreement with Figure 2, the oscillations around 5.9 Hz (the center of the region of common significance) were strong in both ears;  $A = 0.06$  for the left ear, and  $A = 0.05$  for the right ear. Figures 3B and 3F show the 2D

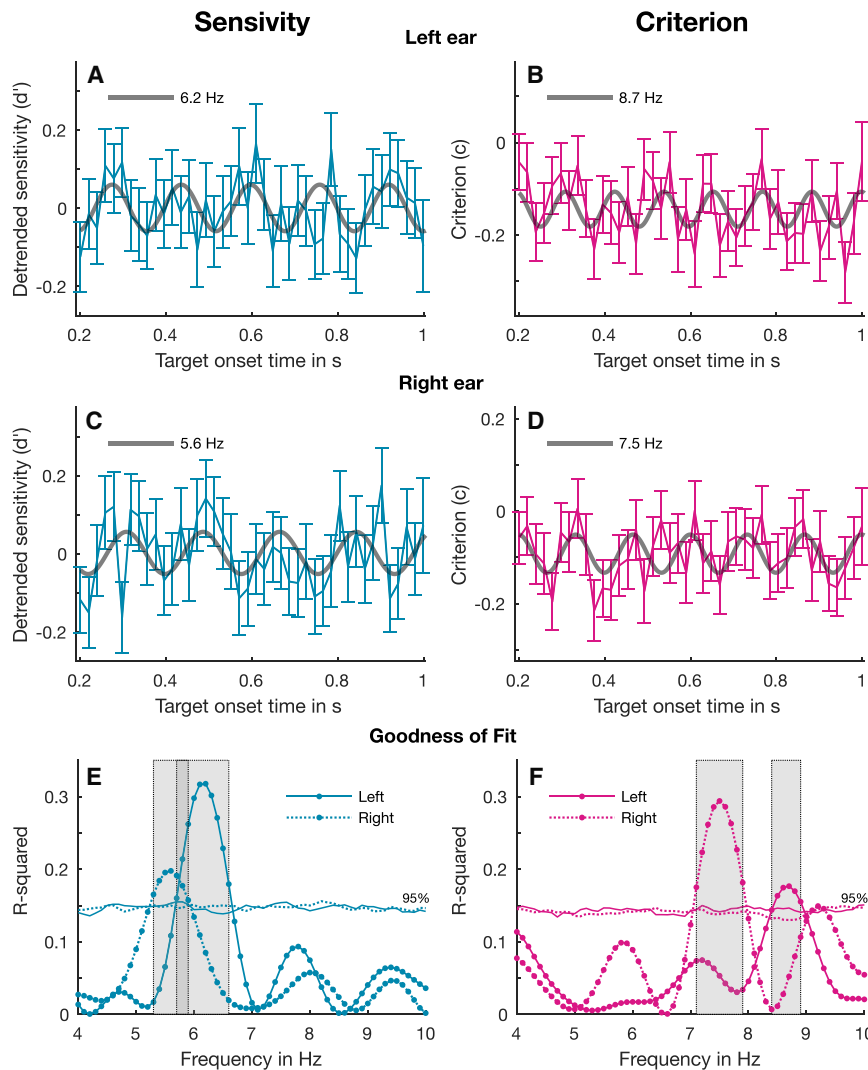


**Figure 2. Best Fourier Model Fits of the Aggregate Subject Sensitivity and Criterion Data**

(A and C) Sensitivity ( $d'$ ) aggregate data fitted with a sinusoidal waveform (Equation 3) after detrending. The best fits are indicated by the black curves for the left ear (A) and right ear (C). The binned data are represented by the blue lines, with error bars indicating  $\pm 1$  SEM for all SOAs.

(B and D) Criterion ( $c$ ) data fitted with a sinusoidal waveform. The best fits (black curves) for the left and right ears are indicated in (B) and (D), respectively. The binned data are depicted in pink, with error bars indicating  $\pm 1$  SEM.

(E and F) Goodness of fit ( $R^2$ ) of the best-fitting sinusoids from 4 to 10 Hz to the original sensitivity (E) and criterion (F) data, compared with the 95% permutation threshold of the  $R^2$  obtained with the same fitting procedure applied to the surrogate data. The gray boxes highlight the range of frequencies within which the original  $R^2$  exceeds 95% of the  $R^2$  of the permuted data.

See also Figures S1 and S2.

Fourier plots of the aggregate subject response at the common frequency, 5.9 Hz (black dots). At this frequency, the bootstrap analysis shows that these vectors were significantly different from zero, with  $p = 0.006$  for the left ear and  $p = 0.01$  for the right ear (FDR = 0.1). The shaded gray areas in Figures 3A–3E show the significant frequencies by the 2D analysis (FDR corrected). Again, these results were corroborated by the individual responses, where participants' phases were highly consistent around 5.9 Hz for both ears: left ear ( $p = 0.01$ ),  $\theta = 175^\circ (\pm 43^\circ)$ , and  $|v| = 0.05$ ; and right ear ( $p = 0.05$ ),  $\theta = 317^\circ (\pm 40^\circ)$ , and  $|v| = 0.05$  (Figure S3).

The aggregate phase for the left- and right-ear sensitivities at the common frequency (5.9 Hz) closely resembles that of the group mean,  $187^\circ (\pm 22^\circ)$  and  $319^\circ (\pm 26^\circ)$ , respectively, leading to a phase difference of  $228^\circ (\pm 34^\circ)$ , approximating antiphase. To further probe this antiphase relationship, we conducted a separate analysis of the sum and difference of sensitivities of the two ears. Figure 4A shows the results of the sinusoidal fit for the sum (green dotted lines) and difference (blue solid lines) of left-ear and right-ear sensitivities over the frequency range of 4–10 Hz (in 0.1-Hz steps). At no frequency does the fit of the

summed sensitivity data exceed the 95% permutation threshold, while that of the difference data does so over the range of 5.2–6.7 Hz, with a peak at 5.9 Hz. All this is consistent with the oscillations being near antiphase: if they were in phase, the summed response should be higher than the difference, while, if in quadrature phase ( $90^\circ$ ), they should be similar. Figures 4B and 4D show the fit of a 5.9-Hz sinusoid to the difference and summed sensitivity data, respectively. Figures 4C and 4E show the results of the 2D analysis at 5.9 Hz. The amplitude for the difference data (Figure 4B)

at 5.9 Hz was high ( $A = 0.09$ ), with the 95% confidence circle well separated from the origin (Figure 4C), and significant at  $p = 0.001$  (FDR corrected). On the other hand, the amplitude of the summed responses (Figure 4D) was very low ( $A = 0.04$ ), with the 95% confidence circle clearly encompassing the origin (Figure 4E). The proportion of points falling beyond the origin in the direction orthogonal to the phase angle of the real data was 7% ( $p = 0.07$ ).

We extended this analysis to the individual responses (Figures S2 and S3). Taking the difference between the individual sensitivities of the two ears should reduce the phase scatter between subjects, giving rise to a clearer picture of the phase difference in sensitivity across participants. Thus, Figure S4A shows the tendency of the vectors to cluster around  $180^\circ$ , which is absent in Figure S4B. Figures S4C and S4D shows the results of the intersubject phase coherence analysis. Over a large frequency range (5.6–6.4 Hz), participants show significant phase consistency for the sensitivity difference, whereas the same analysis for the summed sensitivity never approaches significance (Figure S4C). Finally, Figure S4D shows that the intersubject phase coherence at 5.9 Hz for the sensitivity difference is also significant against

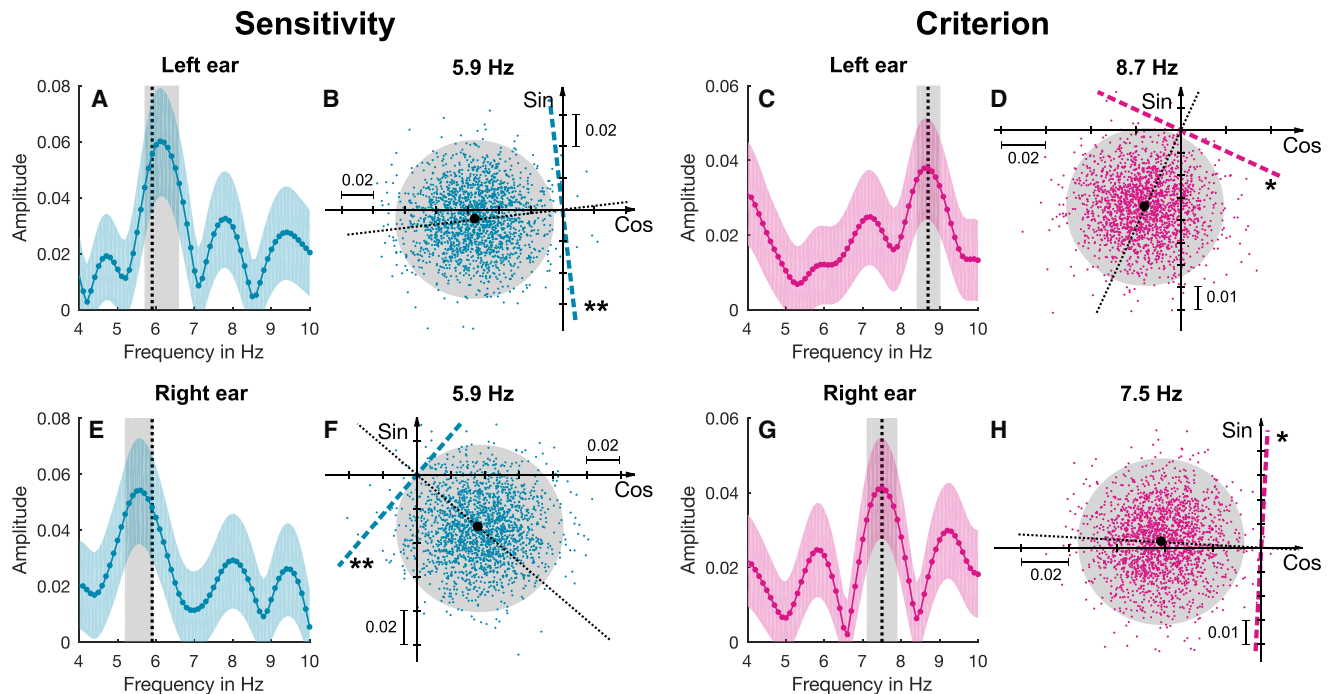


**Figure 3. Amplitude and Phase of the Aggregate Subject Sensitivity and Criterion Data**

(A, B, E, and F) Amplitude spectra of the left-ear (A) and right-ear (E) sensitivities for the 61 frequencies (from 4 Hz to 10 Hz in 0.1-Hz steps). The blue shaded area around the blue lines represents  $\pm 1$  SEM. The gray shaded rectangles show the regions where the 2D bootstrap test was significant. The plots at the right of spectra, in (B) and (F), illustrate the 2D bootstrap tests for 5.9 Hz. The black dots at the center of the gray shaded circles plot the sinusoidal fit of the original data; the smaller blue dots plot that of the bootstrapped data. The gray shaded circles drawn around the bootstrapped distributions indicate the 95% bounds. Asterisks indicate significance, judged from the proportion of the bootstrapped data falling in the semi-plane orthogonal to the phase angle of the original data (dotted lines): \* $p < 0.05$ ; \*\* $p < 0.01$ . All  $p$  values were FDR corrected across 61 frequency bins.

(C, D, G, and H) Amplitude spectra and 2D test results for criterion (pink) in the left ear (C and D) and in the right ear (G and H), in the same format as the left panels. See also [Figure S3](#).

the maximal intersubject phase coherence of the permuted data across all frequencies.

## DISCUSSION

The present study reports, for the first time, oscillations in the perception of auditory stimuli (in the absence of neural entrainment), showing that oscillations in performance are not specific to vision, as has been previously assumed [4, 5], but may reflect a more general perceptual mechanism. Using signal detection theory (SDT), we found that auditory oscillations occur in both sensitivity and criterion, but at different frequencies: 5–6 Hz for sensitivity and 7–8 Hz for criterion. The frequencies are similar but straddle the theta and alpha bands (4–7 Hz and 8–12 Hz, respectively), with sensitivity more in the theta range and criterion more in the alpha range. Both theta and alpha oscillations have been implicated in various attentional processes, and the phases of theta and alpha rhythms are known to modulate the amplitude of higher frequencies, such as gamma (~40–90 Hz), which drives numerous perceptual processes [21–23].

Our observation that the oscillations in sensitivity for pitch discrimination occurred within the theta band is consistent with a recent study [24] showing that the amplitude of theta oscillatory activity in the right inferior frontal gyrus predicted pitch discrimination performance. The oscillations of sensitivity of the two

ears were clearly in antiphase, supported by the fact that the summed responses of both ears showed no significant oscillations, while the differences showed stronger oscillations than for either ear alone, over a range of frequencies (Figure 4). This result agrees with two behavioral studies on oscillation of visual thresholds [2, 3], both showing clear theta modulation of accuracy during a spatially cued task. Importantly, the theta band modulation measured at the two hemifields [2] or between two object locations [3] were in approximate antiphase, implying alternate sampling between them. A similar process may occur in the current study. Our target stimuli were presented to either the left or the right ear, producing maximal interaural differences for auditory lateralization, similar to the presentations in the two visual studies [2, 3]. Sensitivity oscillated at very similar frequencies for the two ears (~6 Hz), approximately in antiphase, in a way similar to that observed in the studies on visual sensitivity, suggesting that oscillations in visual and auditory sensitivity may result from a general attentional mechanism that samples target locations in a cyclic manner. This could be an efficient general strategy for perceptual systems with limited resources [4]. The antiphase relationship between the two ears may also help to explain why previous research has failed to reveal clear auditory oscillations (in the absence of rhythmic entrainment) [6–8]. Most previous research has used diotic stimulus presentation, where identical sounds were presented to both ears

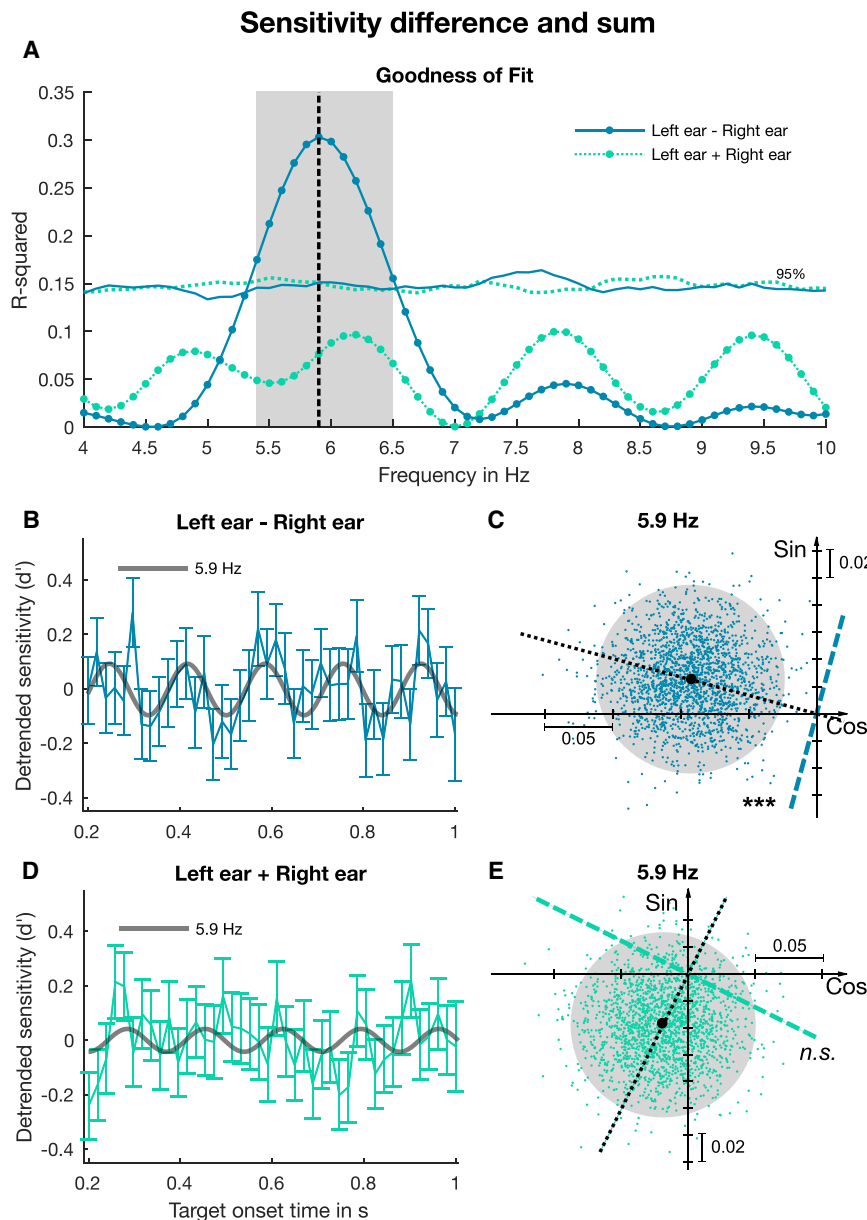


**Figure 4. Fourier Fit, Amplitude, and Phase of the Difference and Sum of Left- and Right-Ear Aggregate Subject Sensitivity**

(A) Goodness-of-fit measures ( $R^2$ ) for the difference (blue solid lines) and sum (green dashed lines) of the left and right ear at 61 tested frequencies from 4 to 10 Hz (in 0.1-Hz steps). The sum and difference were fitted with same Fourier model as in Figure 2. The black dashed line indicates the best-fitting frequency at 5.9 Hz for the sensitivity difference.

(B) Sensitivity difference (blue curve) plotted with the best fitting sinusoid (5.9 Hz).

(C) The results of the 2D bootstrap test for the difference in (B) at the best-fitting frequency. The black and blue dots represent the original and bootstrapped data, respectively. The gray shaded circle includes 95% of the bootstrapped data, and the asterisks indicate the proportion of the bootstrapped data beyond the blue dashed line which passes through the origin and is orthogonal to the phase angle of the aggregate data:  $***p < 0.001$ . All  $p$  values were FDR corrected across 61 frequency bins.

(D) For comparison, the sum of the left-ear and right-ear sensitivities (green curve) is fitted with a 5.9-Hz sinusoid.

(E) The results of the 2D bootstrap test for the summed sensitivity in (C) at 5.9 Hz: not significant (n.s.).

See also Figure S4.

simultaneously. Our results would suggest that, in these situations, potential interaural oscillations would be cancelled out. Indeed, when pooling together our results from the left and right ears, the oscillations cancelled out almost completely (Figure 4D). In a normal listening environment, it is rare for a sound to be completely lateralized to one ear. Future studies should examine whether similar antiphase oscillations are also present in a more naturalistic environment with stimuli that can be localized spatially.

In addition to the oscillations in auditory sensitivity, we report significant oscillations in decision criterion, at 7–8 Hz. A wealth of studies relates the power and phase of alpha rhythms to attention [21–23] and to changes in performance, particularly with visual tasks [1–3, 14, 15, 17]. However, very few studies have attempted to separate sensitivity from criterion. One exception is lemi et al. [25], who reported that reduced alpha activity pre-

dicted a more liberal detection criterion for several visual tasks, but not improved sensitivity, consistent with our results. Several studies give support for this idea for vision [26], touch [27], and even audition [28], although none of these specifically separated sensitivity and criterion. Sherman et al. [29] also used SDT to study oscillations in a visual detection task and showed that the phase of alpha oscillations in the EEG before the stimulus onset predicted criterion (and confidence judgments), but not sensitivity.

Furthermore, when there was high expectation of target appearance (leading to a more liberal criterion) the oscillation was in antiphase with conditions of low expectation, leading the authors to suggest that the alpha band neural oscillations transmit expectation, or priors, to sensory cortex. This idea is supported on theoretical grounds [30] and also by work showing that alpha-band desynchronization predicts temporal expectation effects [31]. In our experiment, the two stimuli were equally probable, leading to no systematic “expectation” for one tone or the other. However, many factors influence expectancies, including the previous stimulus history [32, 33], and this form of expectancy (or prior) may be transmitted by alpha-band communication.

It is far from clear why criteria should oscillate at different frequencies in the two ears, as criteria are usually considered decision boundaries, which may be expected to be set at higher levels of stimulus analysis. However, our data suggest that the

decision boundary of the pitch discrimination is set separately for the two ears or two hemispheres. Perhaps the brain uses a frequency tagging code to simultaneously classify pitch and space localization. Further experimentation would be required to isolate better the mechanisms governing oscillations in criterion.

In conclusion, our study adds to many others in showing that, even under apparently stable conditions, perceptual performance is not constant but oscillates continually. We find that both criterion and sensitivity oscillate, at different frequencies, reflecting different driving mechanisms, both consistent with what has been previously reported in the visual literature. That this occurs for audition as well as vision suggests that it reflects a general perceptual strategy where preceding events can synchronize endogenous brain oscillations to influence the incoming stimulus.

### STAR★METHODS

Detailed methods are provided in the online version of this paper and include the following:

- KEY RESOURCES TABLE
- CONTACT FOR REAGENT AND RESOURCE SHARING
- EXPERIMENTAL MODEL AND SUBJECT DETAILS
- METHODS DETAILS
- QUANTIFICATION AND STATISTICAL ANALYSIS
  - Aggregate Subject Analysis
  - Individual Subject Analysis
- DATA AND SOFTWARE AVAILABILITY

### SUPPLEMENTAL INFORMATION

Supplemental Information includes four figures and one set of individual and aggregate subject data and can be found with this article online at <https://doi.org/10.1016/j.cub.2017.10.017>.

### AUTHOR CONTRIBUTIONS

H.T.H. and J.L. conducted the experiment. M.C.M., D.C.B., D.A., J.L., and H.T.H. designed the experiment and wrote the paper.

### ACKNOWLEDGMENTS

The research was supported by the Australian Research Council Discovery Project (DP150101731) and the European Research Council (FPT/2007-2013) under grant agreement 338866 Ecsplain.

Received: June 30, 2017

Revised: September 15, 2017

Accepted: October 5, 2017

Published: November 16, 2017

### REFERENCES

1. Benedetto, A., Spinelli, D., and Morrone, M.C. (2016). Rhythmic modulation of visual contrast discrimination triggered by action. *Proc. Biol. Sci.* *283*, 20160692.
2. Landau, A.N., and Fries, P. (2012). Attention samples stimuli rhythmically. *Curr. Biol.* *22*, 1000–1004.
3. Fiebelkorn, I.C., Saalman, Y.B., and Kastner, S. (2013). Rhythmic sampling within and between objects despite sustained attention at a cued location. *Curr. Biol.* *23*, 2553–2558.
4. VanRullen, R. (2016). Perceptual cycles. *Trends Cogn. Sci.* *20*, 723–735.
5. VanRullen, R., Zoefel, B., and Ilhan, B. (2014). On the cyclic nature of perception in vision versus audition. *Philos. Trans. R. Soc. Lond. B Biol. Sci.* *369*, 20130214.
6. Zoefel, B., and Heil, P. (2013). Detection of near-threshold sounds is independent of EEG phase in common frequency bands. *Front. Psychol.* *4*, 262.
7. İlhan, B., and VanRullen, R. (2012). No counterpart of visual perceptual echoes in the auditory system. *PLoS ONE* *7*, e49287.
8. Ng, B.S., Schroeder, T., and Kayser, C. (2012). A precluding but not ensuring role of entrained low-frequency oscillations for auditory perception. *J. Neurosci.* *32*, 12268–12276.
9. Neuling, T., Rach, S., Wagner, S., Wolters, C.H., and Herrmann, C.S. (2012). Good vibrations: oscillatory phase shapes perception. *Neuroimage* *63*, 771–778.
10. Hickok, G., Farahbod, H., and Saberi, K. (2015). The rhythm of perception: entrainment to acoustic rhythms induces subsequent perceptual oscillation. *Psychol. Sci.* *26*, 1006–1013.
11. Macmillan, N.A., and Creelman, D.C. (2004). *Detection Theory: A User's Guide* (Erlbaum).
12. Green, D.M., and Swets, J.A. (1966). *Signal Detection Theory and Psychophysics* (Wiley).
13. Harris, A.M., Dux, P.E., Jones, C.N., and Mattingley, J.B. (2017). Distinct roles of theta and alpha oscillations in the involuntary capture of goal-directed attention. *Neuroimage* *152*, 171–183.
14. Huang, Y., Chen, L., and Luo, H. (2015). Behavioral oscillation in priming: competing perceptual predictions conveyed in alternating theta-band rhythms. *J. Neurosci.* *35*, 2830–2837.
15. Song, K., Meng, M., Chen, L., Zhou, K., and Luo, H. (2014). Behavioral oscillations in attention: rhythmic  $\alpha$  pulses mediated through  $\theta$  band. *J. Neurosci.* *34*, 4837–4844.
16. Benedetto, A., and Morrone, M.C. (2017). Saccadic suppression is embedded within extended oscillatory modulation of sensitivity. *J. Neurosci.* *37*, 3661–3670.
17. Tomassini, A., Spinelli, D., Jacono, M., Sandini, G., and Morrone, M.C. (2015). Rhythmic oscillations of visual contrast sensitivity synchronized with action. *J. Neurosci.* *35*, 7019–7029.
18. Phipson, B., and Smyth, G.K. (2010). Permutation P-values should never be zero: calculating exact P-values when permutations are randomly drawn. *Stat. Appl. Genet. Mol. Biol.* *9*, Article39.
19. Benjamini, Y., and Hochberg, Y. (1995). Controlling the false discovery rate: a practical and powerful approach to multiple testing. *J. R. Stat. Soc. B* *57*, 289–300.
20. Genovese, C.R., Lazar, N.A., and Nichols, T. (2002). Thresholding of statistical maps in functional neuroimaging using the false discovery rate. *Neuroimage* *15*, 870–878.
21. Lisman, J.E., and Jensen, O. (2013). The  $\theta$ - $\gamma$  neural code. *Neuron* *77*, 1002–1016.
22. Jensen, O., Gips, B., Bergmann, T.O., and Bonnefond, M. (2014). Temporal coding organized by coupled alpha and gamma oscillations prioritize visual processing. *Trends Neurosci.* *37*, 357–369.
23. Fries, P. (2015). Rhythms for cognition: communication through coherence. *Neuron* *88*, 220–235.
24. Florin, E., Vuvar, D., Peretz, I., and Baillet, S. (2017). Pre-target neural oscillations predict variability in the detection of small pitch changes. *PLoS ONE* *12*, e0177836.
25. Iemi, L., Chaumon, M., Crouzet, S.M., and Busch, N.A. (2017). Spontaneous neural oscillations bias perception by modulating baseline excitability. *J. Neurosci.* *37*, 807–819.
26. Mathewson, K.E., Gratton, G., Fabiani, M., Beck, D.M., and Ro, T. (2009). To see or not to see: prestimulus alpha phase predicts visual awareness. *J. Neurosci.* *29*, 2725–2732.

27. Baumgarten, T.J., Schnitzler, A., and Lange, J. (2016). Prestimulus alpha power influences tactile temporal perceptual discrimination and confidence in decisions. *Cereb. Cortex* *26*, 891–903.
28. Leske, S., Ruhnau, P., Frey, J., Lithari, C., Müller, N., Hartmann, T., and Weisz, N. (2015). Prestimulus network integration of auditory cortex predisposes near-threshold perception independently of local excitability. *Cereb. Cortex* *25*, 4898–4907.
29. Sherman, M.T., Kanai, R., Seth, A.K., and VanRullen, R. (2016). Rhythmic influence of top-down perceptual priors in the phase of prestimulus occipital alpha oscillations. *J. Cogn. Neurosci.* *28*, 1318–1330.
30. Friston, K.J., Bastos, A.M., Pinotsis, D., and Litvak, V. (2015). LFP and oscillations—what do they tell us? *Curr. Opin. Neurobiol.* *31*, 1–6.
31. Rohenkohl, G., and Nobre, A.C. (2011).  $\alpha$  oscillations related to anticipatory attention follow temporal expectations. *J. Neurosci.* *31*, 14076–14084.
32. Fischer, J., and Whitney, D. (2014). Serial dependence in visual perception. *Nat. Neurosci.* *17*, 738–743.
33. Cicchini, G.M., Anobile, G., and Burr, D.C. (2014). Compressive mapping of number to space reflects dynamic encoding mechanisms, not static logarithmic transform. *Proc. Natl. Acad. Sci. USA* *111*, 7867–7872.
34. Brainard, D.H. (1997). The psychophysics toolbox. *Spat. Vis.* *10*, 433–436.
35. Faes, L., Nollo, G., Ravelli, F., Ricci, L., Vescovi, M., Turatto, M., Pavani, F., and Antolini, R. (2007). Small-sample characterization of stochastic approximation staircases in forced-choice adaptive threshold estimation. *Percept. Psychophys.* *69*, 254–262.
36. García-Pérez, M.A. (2011). A cautionary note on the use of the adaptive up-down method. *J. Acoust. Soc. Am.* *130*, 2098–2107.
37. Hautus, M.J. (1995). Corrections for extreme proportions and their biasing effects on estimated values of  $d'$ . *Behav. Res. Methods Instrum. Comput.* *27*, 46–51.
38. Stanislaw, H., and Todorov, N. (1999). Calculation of signal detection theory measures. *Behav. Res. Methods Instrum. Comput.* *31*, 137–149.

## STAR★METHODS

### KEY RESOURCES TABLE

REAGENT or RESOURCE	SOURCE	IDENTIFIER
Software and Algorithms		
MATLAB 2016b	The MathWorks	SCR_001622
Psychophysics Toolbox 3	[34]	SCR_002881
Other		
DATAPixx	Vpixx Technologies	SCR_009648
ResponsePixx	Vpixx Technologies	N/A
Curve Fitting Toolbox	The MathWorks	N/A
ER-2 in-ear tube phones	Etymotic Research	N/A

### CONTACT FOR REAGENT AND RESOURCE SHARING

Further information and requests for resources should be directed to and will be fulfilled by the Lead Contact, David Burr ([dave@in.cnr.it](mailto:dave@in.cnr.it)). There is no restriction for distribution of materials.

### EXPERIMENTAL MODEL AND SUBJECT DETAILS

Twenty healthy adults (7 male, 3 left-handed, mean age  $21.8 \pm 3.9$ ) with normal hearing participated in the experiment. All participants provided written, informed consent. The study was approved by the Human Research Ethics Committees of the University of Sydney.

### METHODS DETAILS

Participants performed a bilateral pitch-identification task within dichotic white noise maskers, delivered via in-ear tube-phones (ER-2, Etymotic Research, Elk Grove, Illinois). To isolate external noise, participants wore earmuffs (30 dBA attenuation) over the tube-phones (3M Peltor). The broadband white noise maskers were of 2 s duration and randomly generated on each trial to prevent entrainment. The left- and right-ear maskers were time-reversed versions of each other such that they were clearly lateralised and uncorrelated. A brief (10 ms) target tone (either 2,000 or 2,500 Hz at random, 50% probability) was presented to one ear (at random, 50% probability) at a stimulus-onset asynchrony (SOA) randomly drawn from an interval of 0.2–1.01 s after noise onset. To familiarise participants with the tones, both tones were played four times each before every block. They indicated via button press (ResponsePixx, Vpixx Technologies, Saint-Bruno, Quebec) whether the tone was of high or low pitch, irrespective of the ear in which it occurred. All participants used their thumb (for low pitch) and index finger (for high pitch) of their dominant hand to respond. For each ear, target intensity was kept around individual thresholds (75%), using an accelerated stochastic approximation staircase procedure [35, 36]. Participants were instructed to respond as soon as possible while the noise masker was still present. The next trial started after a silent inter-trial interval (ITI) of random duration between 1.2–2.2 s. Each participant completed 2100 trials (30 blocks of 70 trials) over several sessions on at least two consecutive days. The first six trials of each block were discarded, as thresholds required some trials to stabilize. Blocks lasted ~5 min with rests after each block. Prior to the experiment, participants completed a practice block of 20 trials with feedback, but no feedback was provided during the experiment. Stimuli were presented using the software *PsychToolbox* [34] in conjunction with *DataPixx* (Vpixx Technologies, Saint-Bruno, Quebec) and MATLAB (Mathworks, Natick, Massachusetts).

### QUANTIFICATION AND STATISTICAL ANALYSIS

#### Aggregate Subject Analysis

We examined the behavioral data pooled across the subjects and ran the same analysis on the individual subjects. The individual results are shown in [Figures S1-4](#). Prior to pooling, trials in which the response occurred before the target onset or after the noise offset were discarded. Further, we eliminated trials for which reaction times (RTs) or target intensities were outside 99% of the individuals' RT and target intensity distribution. The responses were subsequently sorted by SOA and grouped into 42 19.5-ms bins, starting from 0.2 up to 1.01 s post noise onset. The 19.5-ms binning induces a time error,  $s_t$ , of  $\pm 9.5$ ms, corresponding to an error in frequency,  $s_f$ , given by the time error ( $s_t$ ) times the square of the frequency ( $s_f = freq^2 \times s_t$ ). In the range of 4–10 Hz  $s_f$  varies between 0.15 and 0.95 Hz.

We applied signal detection theory (SDT: [11]) to separate *sensitivity* from decision *criterion*, separating the responses to the targets in the left and right ears. For each ear,  $d'$  is given by subtracting the z-transformed false alarm rate in the low-pitch condition from the z-transformed hit rate in the high-pitch condition (Figure 1B) and dividing by root two:

$$d' = [z(H_{high}) - z(FA_{low})] / \sqrt{2} \quad (1)$$

Criterion (c) is given by:

$$c = -0.5 \times [z(H_{high}) + z(FA_{low})]. \quad (2)$$

We corrected for extreme proportions (0 or 1) by applying the log-linear rule, adding 0.5 to both the number of hits and the number of false alarms, and 1 to both the total number of left-target trials and right-target trials [37, 38].

Using MATLAB's *Curve Fitting* toolbox, the sensitivity and criterion data were fitted with a Fourier series model (Figure 2):

$$f(t) = a_0 + a_1 \cos(\omega t) + b_1 \sin(\omega t) = A \cos(\omega t + \phi), \quad (3)$$

where  $t$  is time,  $\omega$  is the frequency,  $a_1$  and  $b_1$  are the cosine and sine coefficients respectively, and  $a_0$  is a constant.  $A$  and  $\phi$  represent amplitude and phase of the sinusoidal fit. We used a non-linear least-squares method whereby the summed squares of the residuals were minimized through successive iterations (400 iterations in total). Before curve fitting, we removed the decreasing trend in both left- and right-ear sensitivity (Figure S1) using a second-order polynomial fit.

For each frequency between 4 and 10 Hz (in 0.1 Hz steps), we fitted the best sinusoid, allowing amplitude and phase to vary (two degrees of freedom). This yielded a measure of goodness of fit ( $R^2$ ) as a function of frequency (Figure 2E-F). We shuffled the responses from each individual trial over all SOAs to generate 2,000 surrogate datasets, which were binned with the same 19.5 ms rectangular, non-overlapping windows, and fitted with the same sinusoidal fit with two degrees of freedom, as the original data. This resulted in a distribution of 2,000  $R^2$  for every frequency from 4 to 10 Hz, against which we compared the original  $R^2$  (95% thresholds in Figure 2E-F). Additionally, we ran a *jackknife* test whereby one subject was removed at a time. After removal, the aggregated data were binned and fitted as described above. The results can be inspected in Figure S2C-D.

To evaluate the amplitude and phase of the criterion and sensitivity oscillations, we applied a two-dimensional (2D) significance test that involved bootstrapping the original data 2,000 times and submitting the bootstrapped data to the same binning and fitting procedure as the original data (with two degrees of freedom). For each condition, we examined the fit of the original data (black dots at the center of the blue and pink clouds), together with that of the bootstrapped data at all 61 frequencies (e.g., Figure 3B). In particular, we calculated the exact proportion of the bootstrapped data that belonged in the semi-plane opposite to the vector of the aggregate data. This is defined by the line passing through the origin and orthogonal to the phase angles of the original data. In practice, this meant the proportion of blue or pink dots (in, e.g., Figure 3B) that fell beyond the dotted colored line. The resulting p values were corrected over all 61 frequency bins using the False Discovery Rate (FDR) method [19]. We set the FDR to the recommended level, 0.1 [20].

Finally, to explore the antiphase difference between the sensitivity in the two ears, we computed the difference between the left-ear and right-ear sensitivity oscillations (Figure 4) by subtracting the right-ear sensitivity bins (Figure 1C, blue curve) from those of the left ear (Figure 1D, blue curve). For comparison, we also summed the left and right ear sensitivity and submitted both the sum and difference to the same fitting procedure, permutation, and bootstrap tests as above. The analysis of the sum and difference in sensitivity was conducted at both the aggregate and individual subject level. The resulting p values were FDR corrected as above.

### Individual Subject Analysis

In addition to the aggregate subject data analysis, we also examined the behavioral data at the individual subject level. To reduce the noise in the individual data, the responses were smoothed with a rectangular window of 26 ms width. The window was moved every 19.5 ms, resulting in 42 overlapping bins, ranging from 0.2 to 1.01 s post noise-onset. The average number of trials per bin per ear was 31 trials at the individual subject level. At the aggregate subject level, the average number of trials per bin per ear was 471 trials. Similar to the aggregate subject analysis (for which we pooled across participants), we obtained two temporal sequences of sensitivity and criterion for every participant, separately for each ear (Figure S1). The sequences were submitted to the same detrending, permutation (200 iterations), bootstrap (200 iterations), and Fourier modeling procedure as the aggregate subject analysis (Equation 3). The individual  $R^2$  can be inspected in Figure S2A-B.

We also examined amplitude and phase for each participant over the frequency range 4-10 Hz in 0.1-Hz steps using the 2D bootstrap test (Figure S3). To investigate the intersubject phase coherence, we computed the mean vector (for the group) and determined the significance of its magnitude (which reflects the coherence of the individual phases scaled by their amplitudes) by permutation test. This is essentially equivalent to the 2D bootstrap test, the difference being that the phase coherence analysis takes the subject variability explicitly into consideration. Crucially, for this test to be significant, two conditions must be met. First, the group mean amplitude exceeds that of the permuted data and, second, the phase coherence across subjects is greater than that of the permuted data. The reported p values (see Results) reflect the proportion of permutations greater or equal the phase coherence of the original data.

Finally, we also inspected the individual phase angle difference between left- and right-ear sensitivity at the common frequency, 5.9 Hz. As in the aggregate data analysis, we subtracted the individual right sensitivity from the left one bin by bin. For comparison, we also summed the individual right and left sensitivity. To test whether all participants show the observed antiphase difference in sensitivity, we applied the same individual subject and intersubject phase coherence analysis as above ([Figure S4](#)).

#### **DATA AND SOFTWARE AVAILABILITY**

For data analysis, we used off-the-shelf routines available in MATLAB (version R2016b) in combination with the MATLAB Curve Fitting toolbox. Our individual and aggregate subject dataset is available in Excel format as [Data S1](#).